Franklin Open 5 (2023) 100052

Contents lists available at ScienceDirect

Franklin Open

journal homepage: www.elsevier.com/locate/fraope

Sliding mode consensus control for multi-agent systems under multi-node round-robin protocol

Jiancheng Xu, Yugang Niu *

Key Laboratory of Smart Manufacturing in Energy Chemical Process (East China University of Science and Technology), Ministry of Education, Shanghai, 200237, China

ARTICLE INFO

Keywords:
Multi-agent systems
Consensus
Multi-node round-robin protocol
Sliding mode control

ABSTRACT

This work investigates the consensus issue for nonlinear multi-agent systems (MASs) via the multi-node round-robin protocol (MRRP) and sliding mode control (SMC) method. The MRRP is used to schedule information transmissions among agents. On the one hand, considering the limited communication ability of the leader, the leader could take turns sending information to several nearby followers. On the other hand, for reasonably scheduling communication resources among followers, the number of follower's sensor nodes could be automatically adjusted to transmit their information according to the size of the consensus error. Under the MRRP, a token-dependent sliding mode controller is designed to achieve consensus. And controller gains are obtained via the optimized algorithm. Eventually, two numerical simulation instances are furnished to substantiate the efficacy of the proposed SMC strategy under MRRP.

1. Introduction

With the rapid development of information interaction technology, multi-agent systems (MASs) have become the key technology to solve complex problems and realize intelligence and have received more and more scholars' attention and have been widely used, such as intelligent transportation [1], industrial automation [2], microgrid [3], aerospace [4] and so on. As one of the focal areas in MASs, consensus is the agreement or action of all agents in the course of cooperation to achieve the overall mission goals. An embedded control scheme was introduced in [5] that utilizes a signal generator to achieve the optimal output consensus of the MASs network. The adaptive event-triggered consensus was considered in [6] for the MASs on undirected graphs without and with external disturbances. The finite-time leader-following consensus of the second-order MASs was investigated in [7] via event-triggered communication.

Sliding mode control (SMC) is a nonlinear control method with strong robustness to uncertainties and disturbances, and has been widely used [8–12]. Its key characteristic is its ability to effectively suppress model uncertainties and disturbances. For example, the sliding mode finite-time consensus tracking problem of MASs with uncertain follower states in the presence of actuator attacks was investigated in [11]. An event-triggered sliding mode controller was proposed for the scaled consensus of MASs in [12].

However, with the increasing complexity of systems, frequent data exchanges and the scarcity of network resources in MAS present numerous challenges, such as network congestion, data conflicts, and soaring communication costs. Therefore, the rational scheduling of network resources for every agent has become an immensely significant research subject. Network scheduling protocols offer a promising approach to address these issues and have attracted more and more scholars' attention [13–16]. Among the myriad of protocols available, the round-robin (RR) protocol stands out as a readily implementable static scheme [16–22]. Under the RR protocol, when multiple nodes require access to network to transmit information, each node takes turns acquiring a token, granting network access exclusively to the token holder at any given moment. Here, the concept of node is used in the abstract sense, that is, it can refer to the actual sensor node [20–22], or an agent [16–19] in the network.

For example, the static output-feedback SMC problem for uncertain control systems with round-robin protocol scheduling is addressed in [20], where only one actuator node has access to the transmission network at a time. The problem of consensus control of a category of MASs affected by stochastic noise and external disturbances was considered in [22], where the data from the output nodes of each agent is conveyed via a communication network under RR protocol. The H_∞ consensus issue was investigated in [17] for an uncertain discrete time-varying MASs, and the RR protocol was adopted to schedule communication permissions for neighbour agents, under which only one neighbour is allowed to communicate with the agent i at each moment, i.e., agent i cannot receive information from two or

* Corresponding author.
E-mail address: acniuyg@ecust.edu.cn (Y. Niu).

https://doi.org/10.1016/j.fraope.2023.100052
Received 30 August 2023; Received in revised form 18 October 2023; Accepted 13 November 2023
Available online 18 November 2023

more neighbours simultaneously. The problem of the finite-horizon H_∞ bipartite consensus control is investigated in [19] for a class of time-varying cooperation-competition MASs with the RR protocol, where only one neighbouring agent is authorized to transmit the data packet at each time instant to prevent the data collision, too.

Therefore, the RR protocol can reduce the network burden, but it is obvious that enabling the network access for only one node at any given moment greatly limits the information interaction in MASs, especially when an agent (such as a leader) needs to send information to lots of neighbouring agents simultaneously. In addition, may it adjust more than one sensor node of an agent (such as a follower) to access the network? In the process of scheduling, how to deal with these two problems reasonably is a topic worth thinking about.

Compared to the traditional RR protocol mentioned above, the multi-node round-robin protocol (MRRP) has attracted increasing attention [23,24] due to the fact that it allows multiple nodes to transmit information at each moment, rather than just one node. The MRRP was first proposed in [23] for the packet length-dependent lossy network. The probabilistic-constrained control problem of interval type-2 T-S fuzzy systems under the MRRP was considered in [24]. Apparently, the MRRP can schedule network resources more flexibly than the conventional RR protocol.

Inspired by the discussion above, the SMC method is applied to address the consensus tracking issue within leader-following MASs in this work, and a token-dependent distributed SMC law is formulated. The MRRP is utilized to schedule information transmissions of the leader and the followers. The following are the work's main contributions:

(1) A consensus tracking error system model for leader–follower MASs under MRRP is developed to schedule the network resources of the agents.

(2) The leader could take turns sending information to several nearby followers. For each follower, the access number of sensor nodes can be adjusted flexibly under the MRRP.

(3) Both the asymptotic stability of the closed-loop system and the reachability of the sliding surface are analysed, and the optimization problem along with its respective solving algorithm is provided.

Notation. I_n is an n-order identity matrix. $\otimes$ denotes the Kronecker product. $\alpha_{\min}(A)$ represents the minimum eigenvalue of A. $\mathrm{sgn}(\cdot)$ denotes the standard sign function. $\mathbf{1}_N$ represents an N-dimensional vector $[1, 1, \ldots, 1]^T$.

2. Preliminaries

2.1. Graph theory

A directed graph $\mathcal{G}$ consists of a pair (ν, ζ), where $\zeta \in \nu \times \nu$ and $\nu = \{1, 2, \ldots, N\}$. The nodes ν and edges ζ in graph $\mathcal{G}$ represent agents and communication channels among agents, respectively. A directed graph has a directed spanning tree when there is a root node with a directed path to every other node.

Define $R = \mathrm{diag}\{r_1, r_2, \ldots, r_N\}$ to represent the communication between all followers and the leader. If follower i can receive messages from the leader, $r_i > 0$, otherwise, $r_i = 0$. Define the adjacency matrix in graph $\mathcal{G}$ as $H = [h_{ij}] \in \mathbb{R}^{N\times N}$. If the edge $(j, i) \in \zeta$, $h_{ij} > 0$ means that agent i can receive information from agent j, otherwise, $h_{ij} = 0$. The in-degree of node ν_i in the graph $\mathcal{G}$ is defined as $d_i = \sum_{j=1}^{N} h_{ij}$. The Laplacian matrix is defined as $L = D - H$, where $D = \mathrm{diag}\{d_1, d_2, \ldots, d_N\}$. The directed graph $\hat{\mathcal{G}}$ is defined to describe the communication relationships among all agents, encompassing both the leader and the followers. It is assumed that the MASs considered in this work contain a directed spanning tree at every instant.

2.2. MRRP

For the traditional RR protocol scheduling, the nodes access the network one by one in a circle to save and schedule communication resources. That is, only one node can transmit information through the network at each instant (as shown in Fig. 1(a)). Define $\Phi(k) \in \{1, \ldots, q\}$ as the token. Under the traditional RR protocol, one has

$$\Phi(k) = \mathrm{mod}(k - 1, q) + 1. \tag{1}$$

While under the MRRP (as shown in Fig. 1(b)), p $(1 \le p \le q)$ nodes at each moment could access the network. Moreover, the first node among these p nodes could obtain the token $\phi(k)$ at k instant via the subsequent updating rule:

$$\phi(k) = \begin{cases} 1, & k = 1 \\ \mathrm{mod}(\phi(k-1) + p - 1, q) + 1, & k \ge 2. \end{cases} \tag{2}$$

Then define all nodes that have permission to access network at k instant as $\psi_a(k)$ $(a = 1, \ldots, p)$, which can be obtained by

$$\psi_a(k) = \begin{cases} \phi(k), & a = 1 \\ \mathrm{mod}(\psi_{a-1}(k), q) + 1, & a = 2, \ldots, p. \end{cases} \tag{3}$$

Remark 1. It can be seen that the update rules (2) of tokens $\phi(k)$ are not only related to k like RR protocol (1), but also to the number p of nodes communicating at each time and the tokens $\phi(k-1)$ from the previous time. When p reduces to 1, the MRRP becomes the classic RR protocol. Therefore, compared with the classical RR protocol, the MRRP considered in this work is more general. Furthermore, it should be noted that when p is not designed to be a fixed value, e.g., for time-varying $p(k)$, the number of nodes accessing the network in turn can be automatically adjusted according to actual requirements.

2.3. MAS under the MRRP

Consider a MAS composed of a leader and N followers. The leader (agent 0) is modelled as

$$x_0(k+1) = Ax_0(k) + B(u_0(k) + f_0(k)), \tag{4}$$

where $x_0 \in \mathbb{R}^n$ and $u_0 \in \mathbb{R}^m$ are, respectively, the state and control of the leader, $f_0(k)$ is the disturbance.

The dynamic model of the follower i $(i \in \{1, \ldots, N\})$ is given as

$$x_i(k+1) = Ax_i(k) + B(u_i(k) + f_i(k)), \tag{5}$$

where $x_i \in \mathbb{R}^n$, $u_i \in \mathbb{R}^m$, and $f_i(k)$ are the state, control, and disturbance of the ith follower, respectively.

Assumption 1. Assume the disturbances in (4) and (5) satisfy the following Lipschitz condition:

$$\|f_i(k) - f_0(k)\| \le \mu \|x_i(k) - x_0(k)\|. \tag{6}$$

Define the state error between the leader and the follower i as:

$$e_i(k) = x_i(k) - x_0(k). \tag{7}$$

The compact form of the state error can be defined as

$$e(k) = x(k) - \mathbf{1}_N \otimes x_0(k) \tag{8}$$

with $x(k) \triangleq [{x_1}^T(k), \ldots, {x_N}^T(k)]^T$.

In order to attain the objective of enabling each follower to track the leader, we initially establish the consensus tracking error pertaining to the ith follower:

$$\varepsilon_i(k) = \sum_{j=1}^{N} h_{ij}(x_i(k) - x_j(k)) + r_i(x_i(k) - x_0(k)), \tag{9}$$

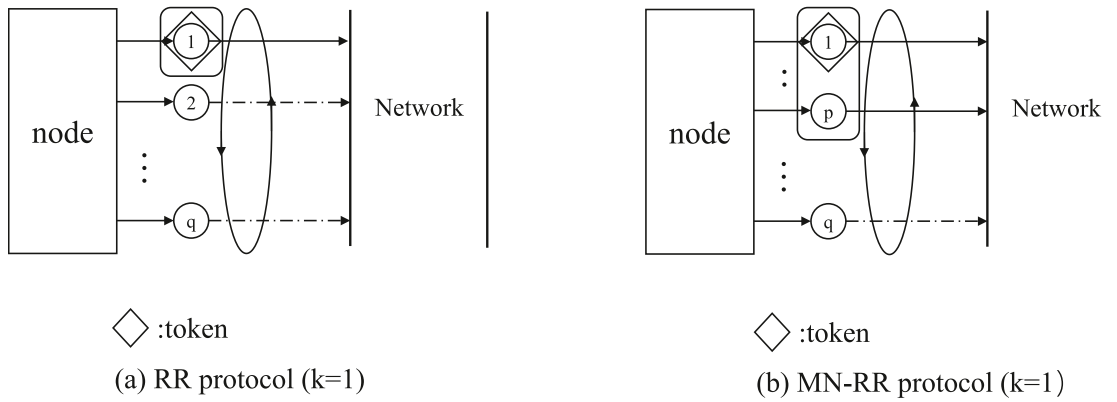

Fig. 1. RR protocol and MRRP.

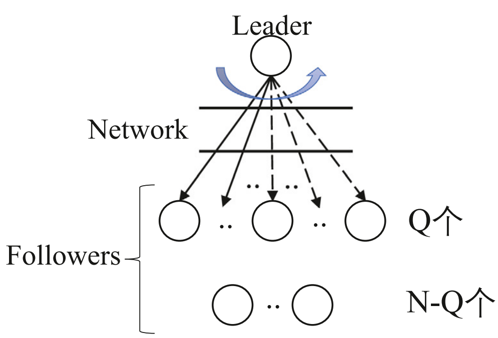

Fig. 2. The leader under the MRRP.

where h_{ij} and r_i denote the elements within the matrices H and R, respectively.

Subsequently, for all followers, the compact form of the consensus tracking error is given as

$$\varepsilon(k) = (L+R)\otimes I_n e(k) \tag{10}$$

with $\varepsilon(k) \triangleq [\varepsilon_1{}^T(k),\dots,\varepsilon_N{}^T(k)]^T$.

According to (10), when $e(k)$ tends to 0, $\varepsilon(k)$ would tend to 0. When $\varepsilon(k)$ approaches 0, the states of all follower agents will become consistent with the leader. In light of this, our control objective is to diminish the consensus tracking error $\varepsilon(k)$ through designing a well-suited SMC law.

In MAS, the leader would send information to multiple neighbour followers. In order to reduce communication burden of the leader and balance the priority of each follower receiving information, the above MRRP is considered to be used between the leader and its neighbour followers.

As shown in Fig. 2, Suppose that there are Q $(1 \le Q \le N)$ followers in the MAS that can directly receive the leader's information, and the remaining $N-Q$ followers cannot. The leader under the MRRP would send information to p of the Q followers at each time.

According to (2), define that the first follower among these p followers could obtain the token $\hat{\phi}(k)$ $(\hat{\phi}(k) \in \mathbb{Q} \triangleq \{1,\dots,Q\})$ at k instant with the subsequent updating rule:

$$\hat{\phi}(k) = \begin{cases} 1, & k=1 \\ \mathrm{mod}(\hat{\phi}(k-1)+p-1,Q)+1, & k \ge 2. \end{cases} \tag{11}$$

From (3), define all followers that have permission to access network at k instant as $\hat{\psi}_a(k)$ $(a=1,\dots,p)$, which can be obtained by

$$\hat{\psi}_a(k) = \begin{cases} \hat{\phi}(k), & a=1 \\ \mathrm{mod}(\hat{\psi}_{a-1}(k),Q)+1, & a=2,\dots,p. \end{cases} \tag{12}$$

Then, under the MRRP, the consensus tracking error (9) of the ith follower is transformed into the following form:

$$\hat{\varepsilon}_i(k) = \sum_{j=1}^{N} h_{ij}(x_i(k)-x_j(k)) + r_i\delta_i^{\hat{\phi}(k)}(x_i(k)-x_0(k)), \tag{13}$$

where $\delta_i^{\hat{\phi}(k)}=1$ when exists $\hat{\psi}_a(k)=i$, and $\delta_i^{\hat{\phi}(k)}=0$ otherwise.

Note that, there is also frequent information exchange among the followers in MAS. With the intention of reducing communication costs of followers and avoid data conflict, the MRRP is considered to schedule the information transmission among followers.

Different from the leader's scheduling mentioned above, among followers, we use MRRP to schedule the components of the transmitted state information $x_i(k)$ $(x_i(k) = [x_{i1}(k),\dots,x_{in}(k)])$. Specifically, this protocol (as shown in Fig. 3) is employed to determine which sensor nodes possess the privilege to transmit their components via the network at every moment, where $p_i(k)$ $(p_i(k) \in \mathbb{N} \triangleq \{1,\dots,n\})$ state components will be sent by the follower i to other followers at k instant. And $\bar{x}_i(k) \triangleq [\bar{x}_{i1}(k),\dots,\bar{x}_{in}(k)]^T$ represents the available signal for the neighbour followers. Define $p_i(1)=n$.

For agent i, define that the first node among these $p_i(k)$ nodes could obtain the token $\bar{\phi}_i(k)$ $(\bar{\phi}_i(k) \in \mathbb{N})$ with the following updating rule at k instant:

$$\bar{\phi}_i(k) = \begin{cases} 1, & k=1 \\ \mathrm{mod}(\bar{\phi}_i(k-1)+p_i(k)-1,n)+1, & k \ge 2, \end{cases} \tag{14}$$

where $p_i(k)$ will be designed later.

For follower i, define all nodes that have permission to access network at k instant as $\bar{\psi}_{i,a}(k)$ $(a=1,\dots,p_i(k))$, which can be obtained by

$$\bar{\psi}_{i,a}(k) = \begin{cases} \bar{\phi}_i(k), & a=1 \\ \mathrm{mod}(\bar{\psi}_{i,a-1}(k),n)+1, & a=2,\dots,p_i(k). \end{cases} \tag{15}$$

Then, for follower i, the available signal for its neighbour followers at the current instant k is represented as

$$\bar{x}_i(k) = \Delta_{\bar{\phi}_i(k)} x_i(k), \tag{16}$$

where $\Delta_{\bar{\phi}_i(k)} \triangleq \mathrm{diag}\{\delta_1^{\bar{\phi}_i(k)},\dots,\delta_n^{\bar{\phi}_i(k)}\}$, $\delta_b^{\bar{\phi}_i(k)}=1$ when exists $\bar{\psi}_{i,a}(k)=b$, and $\delta_b^{\bar{\phi}_i(k)}=0$ otherwise, $b \in \mathbb{N}$.

Now, suppose that follower i receives information $\bar{x}_j(k)$ $(\bar{x}_j(k) = \Delta_{\bar{\phi}_j(k)} x_j(k))$ from its neighbour followers. It can be seen that some components of the transmitted state information $\bar{x}_j(k)$ may be 0, but all components of $x_i(k)$ of agent i are true values. Thus, if $\bar{x}_j(k)$ is directly substituted into expression (13) for calculation, it would result in inaccurate errors. To obtain accurate consensus errors, the local state $x_i(k)$ should be adjusted in accordance with the scheduling signal of neighbouring agents. Therefore, for follower i, we make modifications

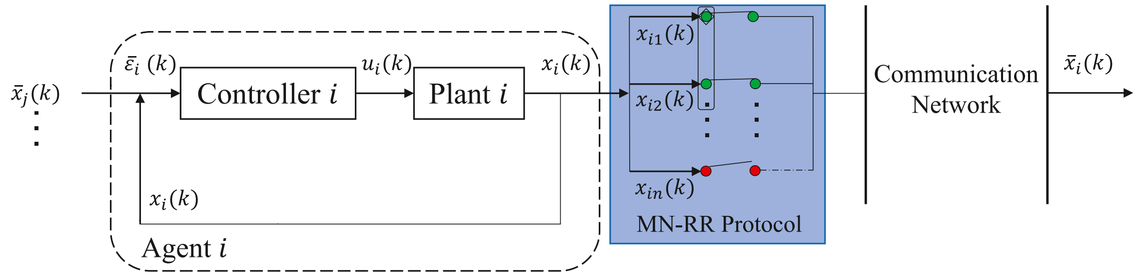

Fig. 3. Follower agents under the MRRP.

to the consensus error (13) and introduce the consensus error model under the MRRP as follows:

$$\bar{\varepsilon}_i(k) = \sum_{j=1}^{N} h_{ij}(\Delta_{\bar{\phi}_j(k)} x_i(k) - \bar{x}_j(k)) + r_i \delta_i^{\hat{\phi}(k)}(x_i(k) - x_0(k)). \tag{17}$$

Then, the number $p_i(k)$ of node information sent by follower i at each time can be defined as follows:

$$p_i(k) = \begin{cases} n, & k = 1 \\ \mathrm{mod}(\lfloor \rho \|\bar{\varepsilon}_i(k-1)\|^2 \rfloor, n) + 1, & k \geq 2, \end{cases} \tag{18}$$

where ρ is a given value.

The consensus error of all followers (17) is given as

$$\bar{\varepsilon}(k) = (L_{\bar{\phi}_f(k)} + R\Lambda_{\hat{\phi}(k)}) \otimes I_n e(k), \tag{19}$$

where $\bar{\varepsilon}(k) \triangleq [\bar{\varepsilon}_1^T(k), \ldots, \bar{\varepsilon}_N^T(k)]^T$, $D_{\bar{\phi}_f(k)} \triangleq \mathrm{diag}\{\bar{d}_1, \ldots, \bar{d}_N\}$, $\bar{d}_i \triangleq \sum_{j=1}^{N} \bar{h}_{ij}$, $H_{\bar{\phi}_f(k)} \triangleq [\bar{h}_{ij}] \in \mathbb{R}^{N\times N}$, $\bar{h}_{ij} \triangleq h_{ij}\Delta_{\bar{\phi}_j(k)}$, $L_{\bar{\phi}_f(k)} \triangleq D_{\bar{\phi}_f(k)} - H_{\bar{\phi}_f(k)}$, $\Lambda_{\hat{\phi}(k)} \triangleq \mathrm{diag}\{\delta_1^{\hat{\phi}(k)}, \ldots, \delta_N^{\hat{\phi}(k)}\}$.

Remark 2. It can be seen that in order to effectively schedule communication resources and flexibly transfer information, we use the MRRP for leader and followers, respectively. For the leader, considering that its communication capacity is limited, we use the MRRP to schedule the targets to which the leader sends information. For the Q neighbouring followers around the leader, the leader sends messages to p of them at each time. So, these Q followers have the same priority to receive messages from the leader under the MRRP. The size of p can be set according to the actual requirements, such as, the communication capacity of the leader, the size of Q, the cost of communication, etc. For each follower, we use the MRRP to schedule its sensor nodes to transmit the information components, that is, the follower i send the component information of $p_i(k)$ nodes to the neighbours at each time in a cyclic form. It should be pointed out that $p_i(k)$(18) here is a dynamic value, and the number of nodes that follower i sends information is related to its consensus error (17) at the previous instant. The smaller the consensus error at the current instant, the smaller the number of nodes which send information at the next instant correspondingly.

2.4. The sliding mode controller design

The sliding function of follower i is constructed as

$$s_i(k) = G_i \varepsilon_i(k), \tag{20}$$

where $G_i \in \mathbb{R}^{m\times n}$ is a given matrix.

Then, the sliding function of all followers could be written as

$$s(k) = G\varepsilon(k) \tag{21}$$

with $s(k) = [s_1(k), \ldots, s_N(k)]^T$, $G \triangleq \mathrm{diag}\{G_1, \ldots, G_N\}$.

The token-dependent SMC law of follower i under the MRRP is designed as

$$u_i(k) = -K_{i,\hat{\phi}(k)}\bar{\varepsilon}_i(k) - \mu\|\bar{\varepsilon}_i(k)\|\mathrm{sgn}(\bar{s}_i(k)) + u_0(k), \tag{22}$$

where the gain $K_{i,\hat{\phi}(k)}$ will be designed later, $\bar{s}_i(k) = G_i\bar{\varepsilon}_i(k)$. Assume that all followers are aware of the leader's control signals, similar as in [25–27]. In subsequent simulations, we will consider two cases in which the control input of the leader is non-zero and zero, respectively.

And then, from (4), (5) and (22), for the follower i, the state error (7) at instant $k+1$ can be calculated as

$$\begin{aligned} e_i(k+1) &= x_i(k+1) - x_0(k+1) \\ &= Ae_i(k) - BK_{i,\hat{\phi}(k)}\bar{\varepsilon}_i(k) + B(f_i(k) - f_0(k)) - \mu B\|\bar{\varepsilon}_i(k)\|\mathrm{sgn}(\bar{s}_i(k)). \end{aligned} \tag{23}$$

The states error of all followers (23) is written as

$$e(k+1) = \tilde{A}e(k) - \tilde{B}K_{\hat{\phi}(k)}\bar{\varepsilon}(k) + \tilde{B}(f(k) - 1_N \otimes f_0(k)) - \mu\tilde{B}\Xi\mathrm{sgn}(\bar{s}(k)), \tag{24}$$

where $e(k+1) = [e_1{}^T(k+1), \ldots, e_N{}^T(k+1)]^T$, $\bar{s}(k) = G\bar{\varepsilon}(k)$, $f(k) = [f_1^T(k), \ldots, f_N^T(k)]^T$, $K_{\hat{\phi}(k)} \triangleq \mathrm{diag}\{K_{1,\hat{\phi}(k)}, \ldots, K_{N,\hat{\phi}(k)}\}$, $\Xi \triangleq \mathrm{diag}\{\|\bar{\varepsilon}_i(k)\|, \ldots, \|\bar{\varepsilon}_N(k)\|\}$, $\tilde{A} \triangleq I_N \otimes A$, $\tilde{B} \triangleq I_N \otimes B$.

From (10), (19), and (24), the consensus error at instant $k+1$ is given as

$$\begin{aligned} \varepsilon(k+1) = &\ (L+R)\otimes I_n e(k+1) \\ = &\ (L+R)\otimes I_n \tilde{A}e(k) - (L+R)\otimes I_n \tilde{B}K_{\hat{\phi}(k)} \\ &\times ((L_{\bar{\phi}_f(k)} + R\Lambda_{\hat{\phi}(k)}) \otimes I_n e(k)) \\ &+ (L+R)\otimes I_n \tilde{B}(f(k) - 1_N \otimes f_0(k)) \\ &+ \mu(L+R)\otimes I_n \tilde{B}\Xi\mathrm{sgn}(\bar{s}(k)) \end{aligned} \tag{25}$$

3. Main results

3.1. Stability analysis

Within this subsection, we derive adequate conditions to ensure the asymptotic stability of the system.

Theorem 1. *Consider the MAS (4)–(5) under the MRRP, for any $i \in \{1, \ldots, N\}$, $\bar{\phi}_i(k) \in \mathbb{N}$, $p_i(k) \in \mathbb{N}$, $\hat{\phi}(k) \in \mathbb{Q}$ and the given positive integer p, and $\rho > 0$, if there exist matrices $P > 0$, $K_{\hat{\phi}(k)}$ and scalar $\alpha > 0$ satisfying*

$$\tilde{B}^T P \tilde{B} \leq \alpha I, \tag{26}$$

$$\begin{aligned} \Psi_1 = &\ 3(\tilde{A} - \tilde{B}K_{\hat{\phi}(k)}((L_{\bar{\phi}_f(k)} + R\Lambda_{\hat{\phi}(k)}) \otimes I_n))^T P(\tilde{A} \\ &+ \tilde{B}K_{\hat{\phi}(k)}((L_{\bar{\phi}_f(k)} + R\Lambda_{\hat{\phi}(k)}) \otimes I_n)) \\ &+ 3\alpha\mu^2 + 3\alpha m\mu^2((L_{\bar{\phi}_f(k)} + R\Lambda_{\hat{\phi}(k)}) \otimes I_n)^T((L_{\bar{\phi}_f(k)} \\ &+ R\Lambda_{\hat{\phi}(k)}) \otimes I_n) - P < 0, \end{aligned} \tag{27}$$

the error system (24) is asymptotically stable.

Proof. The Lyapunov function is constructed as:

$$V_1(k) \triangleq e^T(k)Pe(k), \tag{28}$$

whose difference can be written as

$$\Delta V_1(k) = e^T(k+1)Pe(k+1) - e^T(k)Pe(k). \tag{29}$$

From (19) and (24), we obtain

$$\begin{aligned}&e^T(k+1)Pe(k+1)\\ \leq\ & 3(\tilde{A}-\tilde{B}K_{\hat{\phi}(k)}((L_{\bar{\phi}_f(k)}+R\Lambda_{\hat{\phi}(k)})\otimes I_n)e(k))^T P(\tilde{A}\\ &+\tilde{B}K_{\hat{\phi}(k)}((L_{\bar{\phi}_f(k)}+R\Lambda_{\hat{\phi}(k)})\otimes I_n)e(k))\\ &+3\mu^2(\Xi\mathrm{sgn}(\bar{s}(k)))^T\tilde{B}^T P\tilde{B}\Xi\mathrm{sgn}(\bar{s}(k))\\ &+3(f(k)-1_N\otimes f_0(k))^T\tilde{B}^T P\tilde{B}(f(k)-1_N\otimes f_0(k)).\end{aligned}\tag{30}$$

Based on Assumption 1, we can have:

$$\begin{aligned}\|f(k)-1_N\otimes f_0(k)\| &\leq \|((f_1(k)-f_0(k))^T,\ldots,(f_N(k)-f_0(k))^T)^T\|\\ &\leq \|(\mu\|x_1(k)-x_0(k)\|),\ldots,(\mu\|x_N(k)-x_0(k)\|)\|\\ &\leq \mu\|e(k)\|.\end{aligned}\tag{31}$$

Putting the expressions (26), and (31) into (30) yields

$$\begin{aligned}&e^T(k+1)Pe(k+1)\\ \leq\ & 3e^T(k)(\tilde{A}-\tilde{B}K_{\hat{\phi}(k)}((L_{\bar{\phi}_f(k)}+R\Lambda_{\hat{\phi}(k)})\otimes I_n))^T P(\tilde{A}\\ &+\tilde{B}K_{\hat{\phi}(k)}((L_{\bar{\phi}_f(k)}+R\Lambda_{\hat{\phi}(k)})\otimes I_n))e(k)\\ &+3\alpha\mu^2 e^T(k)e(k)+3\alpha m\mu^2\bar{\varepsilon}^T(k)\bar{\varepsilon}(k)\\ \leq\ & 3e^T(k)(\tilde{A}-\tilde{B}K_{\hat{\phi}(k)}((L_{\bar{\phi}_f(k)}+R\Lambda_{\hat{\phi}(k)})\otimes I_n))^T P(\tilde{A}\\ &+\tilde{B}K_{\hat{\phi}(k)}((L_{\bar{\phi}_f(k)}+R\Lambda_{\hat{\phi}(k)})\otimes I_n))e(k)\\ &+3\alpha\mu^2 e^T(k)e(k)+3\alpha m\mu^2 e^T(k)((L_{\bar{\phi}_f(k)}+R\Lambda_{\hat{\phi}(k)})\otimes I_n)^T((L_{\bar{\phi}_f(k)}\\ &+R\Lambda_{\hat{\phi}(k)})\otimes I_n)e(k).\end{aligned}\tag{32}$$

Thus, by substituting (32) into (29), we obtain

$$\begin{aligned}\Delta V_1(k)\leq\ & 3e^T(k)(\tilde{A}-\tilde{B}K_{\hat{\phi}(k)}((L_{\bar{\phi}_f(k)}+R\Lambda_{\hat{\phi}(k)})\otimes I_n))^T P(\tilde{A}\\ &+\tilde{B}K_{\hat{\phi}(k)}((L_{\bar{\phi}_f(k)}+R\Lambda_{\hat{\phi}(k)})\otimes I_n))e(k)\\ &+3\alpha m\mu^2 e^T(k)((L_{\bar{\phi}_f(k)}+R\Lambda_{\hat{\phi}(k)})\otimes I_n)^T((L_{\bar{\phi}_f(k)}\\ &+R\Lambda_{\hat{\phi}(k)})\otimes I_n)e(k)+3\alpha\mu^2 e^T(k)e(k)\\ &-e^T(k)Pe(k)\\ \leq\ & e^T(k)\Psi_1 e(k).\end{aligned}\tag{33}$$

So, if condition (27) is feasible, we could have $\Delta V_1(k)<0$. Then the system (24) is asymptotically stable, which implies that the MAS (4)–(5) could attain consensus under the MRRP. □

3.2. Reachability analysis

This subsection shows that the state trajectory of the system (24) has the capability converge to a sliding mode domain under the token-dependent controller (22).

Theorem 2. *Consider the MAS (4)–(5) under the MRRP, for any $i\in\{1,\ldots,N\}$, $\bar{\phi}_i(k)\in\mathbb{N}$, $p_i(k)\in\mathbb{N}$, $\hat{\phi}(k)\in\mathbb{Q}$ and the given positive integer p, and $\rho>0$, if there exist matrices $P>0$, $Q>0$, $K_{\hat{\phi}(k)}$ and scalar $\alpha>0$, $\beta>0$ satisfying the conditions (34), (35) and:*

$$(\tilde{B})^T((L+R)\otimes I_n)^T G^T QG((L+R)\otimes I_n)\tilde{B}\leq\beta I,\tag{34}$$

$$\begin{aligned}\Psi_2=\ & 3(G((L+R)\otimes I_n)\tilde{A}-G((L+R)\otimes I_n)\tilde{B}K_{\hat{\phi}(k)}((L_{\bar{\phi}_f(k)}\\ &+R\Lambda_{\hat{\phi}(k)})\otimes I_n))^T Q\\ &\times(G((L+R)\otimes I_n)\tilde{A}-G((L+R)\otimes I_n)\tilde{B}K_{\hat{\phi}(k)}\\ &\times((L_{\bar{\phi}_f(k)}+R\Lambda_{\hat{\phi}(k)})\otimes I_n))\\ &+3\beta ma^2((L_{\bar{\phi}_f(k)}+R\Lambda_{\hat{\phi}(k)})\otimes I_n))^T((L_{\bar{\phi}_f(k)}+R\Lambda_{\hat{\phi}(k)})\otimes I_n))\\ &+\Psi_1<0,\end{aligned}\tag{35}$$

the consensus error's state trajectories will converge to the specified domain Θ:

$$\Theta\triangleq\{s(k)|\|s(k)\|\leq\mu\sqrt{\frac{3\beta}{\alpha_{\min}(Q)}}\|e(k)\|.\tag{36}$$

Proof. The Lyapunov function is chosen as:

$$V_2(k)\triangleq V_1(k)+s^T(k)Qs(k),\tag{37}$$

where $V_1(k)$ defined as in (28).

We obtain from the sliding function (21) and (25)

$$\begin{aligned}s(k+1)=\ & G((L+R)\otimes I_n)\tilde{A}e(k)-G((L+R)\otimes I_n)\tilde{B}K_{\hat{\phi}(k)}\\ &\times((L_{\bar{\phi}_f(k)}+R\Lambda_{\hat{\phi}(k)})\otimes I_n)e(k)\\ &+G((L+R)\otimes I_n)\tilde{B}(f(k)-1_N\otimes f_0(k))\\ &+\mu G((L+R)\otimes I_n)\tilde{B}\Xi\mathrm{sgn}(\bar{s}(k)).\end{aligned}\tag{38}$$

Then, from (31) and (34), we obtain

$$\begin{aligned}&s^T(k+1)Qs(k+1)\\ \leq\ & 3((G((L+R)\otimes I_n)\tilde{A}-G((L+R)\otimes I_n)\tilde{B}K_{\hat{\phi}(k)}\\ &\times((L_{\bar{\phi}_f(k)}+R\Lambda_{\hat{\phi}(k)})\otimes I_n))e(k))^T Q\\ &\times(G((L+R)\otimes I_n)\tilde{A}-G((L+R)\otimes I_n)\tilde{B}K_{\hat{\phi}(k)}\\ &\times((L_{\bar{\phi}_f(k)}+R\Lambda_{\hat{\phi}(k)})\otimes I_n))e(k)\\ &+3(f(k)-1_N\otimes f_0(k))^T(G((L+R)\otimes I_n)\tilde{B})^T QG((L+R)\otimes I_n)\tilde{B}(f(k)\\ &+1_N\otimes f_0(k))\\ &+3\mu^2(\Xi\mathrm{sgn}(\bar{s}(k)))^T(G((L+R)\otimes I_n)\tilde{B})^T QG((L+R)\otimes I_n)\tilde{B}\Xi\mathrm{sgn}(\bar{s}(k))\\ \leq\ & 3e^T(k)(G((L+R)\otimes I_n)\tilde{A}-G((L+R)\otimes I_n)\tilde{B}K_{\hat{\phi}(k)}\\ &\times((L_{\bar{\phi}_f(k)}+R\Lambda_{\hat{\phi}(k)})\otimes I_n))^T Q\\ &\times(G((L+R)\otimes I_n)\tilde{A}-G((L+R)\otimes I_n)\tilde{B}K_{\hat{\phi}(k)}\\ &\times((L_{\bar{\phi}_f(k)}+R\Lambda_{\hat{\phi}(k)})\otimes I_n))e(k)\\ &+3\beta\mu^2\|e(k)\|^2+3m\beta\mu^2 e^T(k)((L_{\bar{\phi}_f(k)}+R\Lambda_{\hat{\phi}(k)})\otimes I_n)^T\\ &\times((L_{\bar{\phi}_f(k)}+R\Lambda_{\hat{\phi}(k)})\otimes I_n)e(k).\end{aligned}\tag{39}$$

Using the expressions (33) and (39), we obtain

$$\begin{aligned}\Delta V_2(k)\leq\ & \Delta V_1(k)+s^T(k+1)Qs(k+1)-s^T(k)Qs(k)\\ \leq\ & e^T(k)(\Psi_1+3(G((L+R)\otimes I_n)\tilde{A}-G((L+R)\otimes I_n)\tilde{B}K_{\hat{\phi}(k)}\\ &\times((L_{\bar{\phi}_f(k)}+R\Lambda_{\hat{\phi}(k)})\otimes I_n))^T Q\\ &\times(G((L+R)\otimes I_n)\tilde{A}-G((L+R)\otimes I_n)\tilde{B}K_{\hat{\phi}(k)}\\ &\times((L_{\bar{\phi}_f(k)}+R\Lambda_{\hat{\phi}(k)})\otimes I_n))-P\\ &+3\beta m\mu^2((L_{\bar{\phi}_f(k)}+R\Lambda_{\hat{\phi}(k)})\otimes I_n)^T((L_{\bar{\phi}_f(k)}+R\Lambda_{\hat{\phi}(k)})\otimes I_n))e(k)\\ &+3\beta\mu^2\|e(k)\|^2-\alpha_{\min}(Q)\|s(k)\|^2\end{aligned}\tag{40}$$

In accordance with the conditions (35), when $\|s(k)\|>\mu\sqrt{\frac{3\beta}{\alpha_{\min}(Q)}}\|e(k)\|$, it results in $\Delta V_2(k)<0$. This implies that the trajectory of the consensus error would converge towards the region Θ. □

It is worth noting that the reachability conditions and the stability conditions of the closed-loop MASs could be guaranteed concurrently by (26), (34), and (35). Nevertheless, it is challenging to get a suitable controller via resolving the nonlinear inequalities directly in Theorem 2 due to the co-existence of matrices P and P^{-1}. To address this issue, a minimization problem that encompasses LMI conditions will be formulated through the subsequent CCL algorithm [28].

Theorem 3. *Consider the MAS (4)–(5) under the MRRP, for any $i\in\{1,\ldots,N\}$, $\bar{\phi}_i(k)\in\mathbb{N}$, $p_i(k)\in\mathbb{N}$, $\hat{\phi}(k)\in\mathbb{Q}$ and the given positive integer p, and $\rho>0$, if the subsequent minimization problem can be solved:*

$$\min_{\bar{P},\bar{Q},P,K_{\hat{\phi}(k)},\alpha,\beta}\mathrm{tr}[P\bar{P}],\tag{41}$$

subject to the conditions:

$$\begin{bmatrix}\bar{\Psi}_{11} & *\\ \bar{\Psi}_{21} & \bar{\Psi}_{22}\end{bmatrix}<0,\tag{42}$$

$$\begin{bmatrix}P & I\\ I & \bar{P}\end{bmatrix}>0,\tag{43}$$

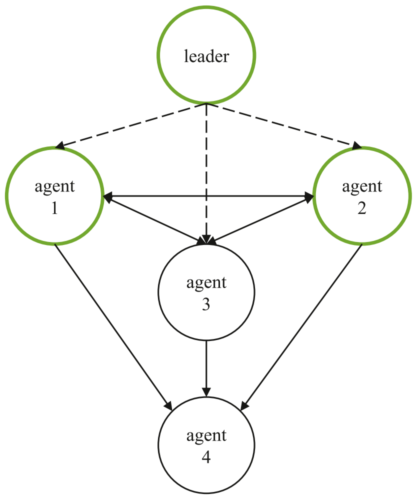

Fig. 4. Communication topology among agents.

$$\begin{bmatrix} -\alpha I & * \\ \tilde{B} & -\bar{P} \end{bmatrix} < 0, \begin{bmatrix} -\beta I & * \\ G((L+R)\otimes I_n)\tilde{B} & -\bar{Q} \end{bmatrix} < 0, \tag{44}$$

with

$$\begin{aligned} \bar{\Psi}_{11} = \ & 3\alpha\mu^2 + 3\alpha m\mu^2((L_{\bar{\phi}_f(k)} + R\Lambda_{\hat{\phi}(k)})\otimes I_n)^T((L_{\bar{\phi}_f(k)} + R\Lambda_{\hat{\phi}(k)})\otimes I_n) - P \\ & + 3\beta m\mu^2((L_{\bar{\phi}_f(k)} + R\Lambda_{\hat{\phi}(k)})\otimes I_n)^T((L_{\bar{\phi}_f(k)} + R\Lambda_{\hat{\phi}(k)})\otimes I_n), \\ \bar{\Psi}_{21} = \ & \begin{bmatrix} \tilde{A} - \tilde{B}K_{\hat{\phi}(k)}((L_{\bar{\phi}_f(k)} + R\Lambda_{\hat{\phi}(k)})\otimes I_n) \\ G((L+R)\otimes I_n)\tilde{A} - G((L+R)\otimes I_n)\tilde{B}K_{\hat{\phi}(k)} \\ \times((L_{\bar{\phi}_f(k)} + R\Lambda_{\hat{\phi}(k)})\otimes I_n) \end{bmatrix}, \\ \bar{\Psi}_{22} = \ & \mathrm{diag}\{-\frac{1}{3}\bar{P}, -\frac{1}{3}\bar{Q}\}, \end{aligned}$$

in such a case, both the asymptotic stability of the system (13) and the specified sliding surface's reachability are accomplished.

Proof. Setting $\bar{P} = P^{-1}$, conditions (42)–(44) could be deduced from conditions (26), (34), and (35). The solution of the minimization problem (41) in Theorem 3 is shown below:

Step 1: Identify a set of admissible solutions $[\bar{P}_0, P_0]$ that meet the requirements (42)–(44). Take $\eta = 0$.

Step 2: Let $\hat{P}_\eta = \bar{P}_\eta$, $\tilde{P}_\eta = P_\eta$ and locate $\bar{P}_{\eta+1}$, $P_{\eta+1}$ via solving the following LMI problem:

$$\min_{\bar{P},\bar{Q},P,K_{\hat{\phi}(k)},\alpha,\beta} \mathrm{tr}[\tilde{P}_\eta\bar{P} + P\hat{P}_\eta], \tag{45}$$

s.t. the conditions (42)–(44) hold,

Step 3: Let $\eta = \eta + 1$ and go to Step 2, until $\eta > \eta_{\max}$, where $\eta_{\max}$ represents maximum number of iterations.

4. Numerical simulation examples

In this section, two kinds of numerical simulations of different communication topologies are provided to further verify the effectiveness of the proposed method.

4.1. Example 1

In this subsection, consider a MAS (4)–(5) with the following parameters, which composed of four followers ($N = 4$) and one leader as shown in Fig. 4. The green circles denote the agents under the MRRP, and the black circles denote that the agents transmit information normally, which means the MRRP is used for agents 0, 1, and 2:

$$A = \begin{bmatrix} 0.9 & 0.5 \\ -0.3 & 0.8 \end{bmatrix}, \ B = \begin{bmatrix} 0.2 \\ 0.1 \end{bmatrix},$$

$$L = \begin{bmatrix} 2 & -1 & -1 & 0 \\ -1 & 2 & -1 & 0 \\ -1 & -1 & 2 & 0 \\ -1 & -1 & -1 & 3 \end{bmatrix}, \ R = \begin{bmatrix} 1 & 0 & 0 & 0 \\ 0 & 1 & 0 & 0 \\ 0 & 0 & 1 & 0 \\ 0 & 0 & 0 & 0 \end{bmatrix}.$$

The controller of the leader agent is given as $u_0(k) = 0.2\sin(\frac{k}{k+1})$. The parameters in the SMC law are given as (22) with $\mu = 0.1$, $G = \tilde{B}^T$, $\rho = 3$. The agents' initial states are given as $x_0 = [50, 50]^T$, $x_1 = [55, 60]^T$, $x_2 = [55, 55]^T$, $x_3 = [40, 40]^T$, $x_4 = [45, 45]^T$.

Upon solving the optimization problem described in (45), the sliding mode controller gains $K_{\hat{\phi}(k)}$ are achieved and are presented in Table 1, where represent three communication topologies of the MASs under the MRRP as shown in Fig. 5. Specifically, 1 represents that the leader (agent 0) transmits information to followers 1 and 2, 2 represents that the leader transmits information to followers 2 and 3, and 3 represents that the leader transmits information to followers 3 and 1.

Figs. 6–11 display the simulation results with the sliding mode. Fig. 6 shows the trajectories of all agents, where the MAS under the MRRP can achieve consensus tracking. Fig. 7 depicts the scheduling selections of the leader and the follower 1 and 2. Specifically, among the three followers, the leader takes turns selecting two followers to send messages at each moment. For the followers 1 and 2, they will adjust

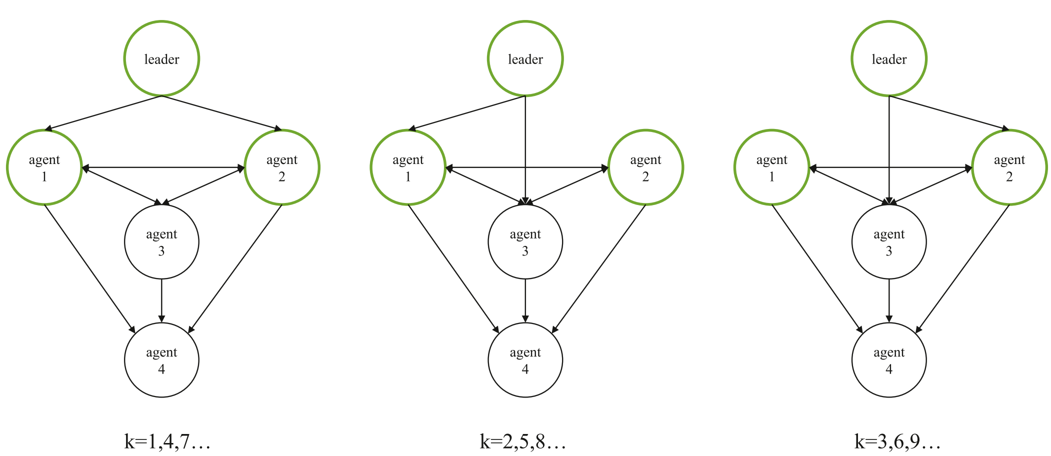

Fig. 5. Communication topology at different times.

Table 1
Sliding mode control gains under MRRP.

Scheduling sequence	Control gains $K_{\hat{\phi}(k)} = \text{diag}\{K_{1,\hat{\phi}(k)}, K_{2,\hat{\phi}(k)}, K_{3,\hat{\phi}(k)}, K_{4,\hat{\phi}(k)}\}$			
$\hat{\phi}(k)$	$K_{1,\hat{\phi}(k)}$	$K_{2,\hat{\phi}(k)}$	$K_{3,\hat{\phi}(k)}$	$K_{4,\hat{\phi}(k)}$
1	[1.7373, 0.5488]	[1.7373, 0.5488]	[1.6645, 0.7963]	[2.4718, 0.7061]
2	[1.6462, 0.5522]	[2.4168, 0.7478]	[0.8929, 0.5973]	[2.4141, 0.7276]
3	[2.4168, 0.7478]	[1.6462, 0.5522]	[0.8929, 0.5973]	[2.4141, 0.7276]

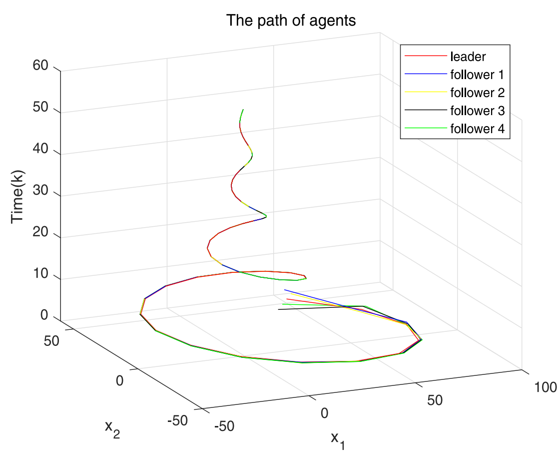

Fig. 6. Motion trajectories.

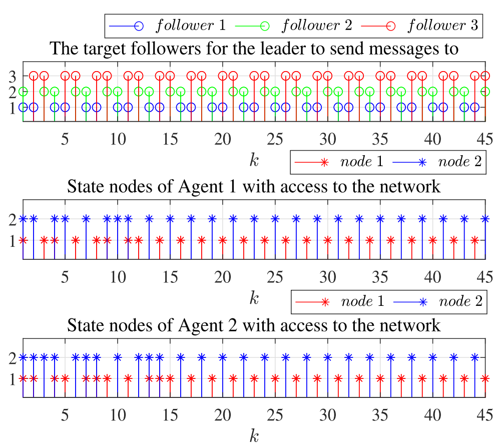

Fig. 7. MRRP scheduling sequence.

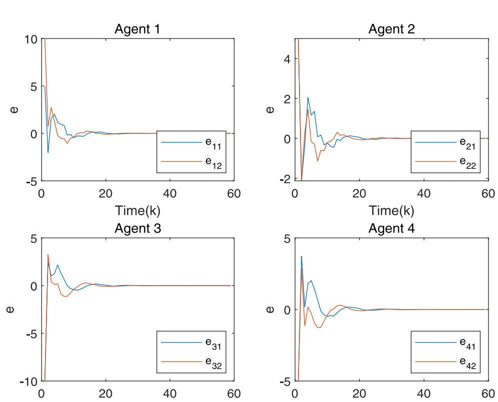

Fig. 8. The state error between the leader and followers.

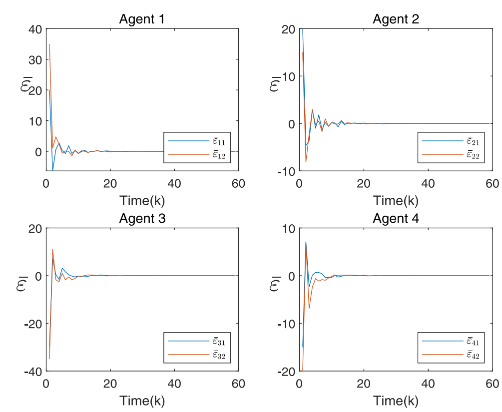

Fig. 9. The consensus error.

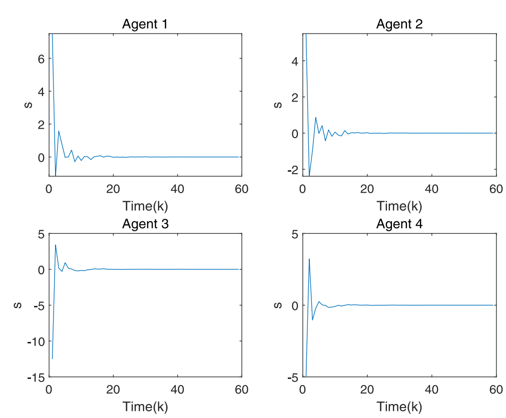

Fig. 10. Sliding variable.

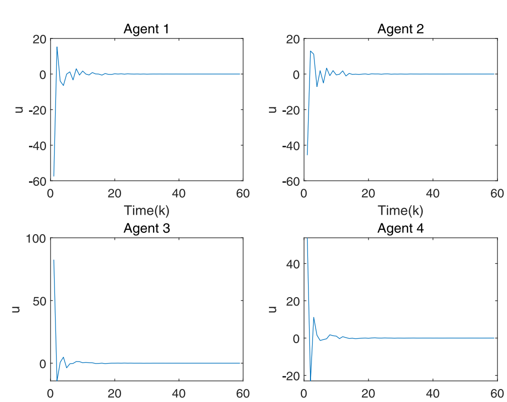

Fig. 11. The control signal of followers.

the number of nodes sending information according to the size of their consensus error. Besides, Fig. 8 shows the state error between leader and each follower. Fig. 9 illustrates the consensus tracking error under the MRRP of the followers. The control signals and sliding variables are depicted in Figs. 10 and 11, respectively.

Table 2
Sliding mode control gains under MRRP.

Scheduling sequence $\hat{\phi}(k)$	Control gains $K_{\hat{\phi}(k)} = \text{diag}\{K_{1,\hat{\phi}(k)}, K_{2,\hat{\phi}(k)}, K_{3,\hat{\phi}(k)}, K_{4,\hat{\phi}(k)}\}$			
	$K_{1,\hat{\phi}(k)}$	$K_{2,\hat{\phi}(k)}$	$K_{3,\hat{\phi}(k)}$	$K_{4,\hat{\phi}(k)}$
1	$[1.5059, -0.0063]$	$[1.2690, 0.0883]$	$[1.8341, 0.0558]$	$[2.0227, -0.0236]$
2	$[2.0227, -0.0236]$	$[1.8341, 0.0558]$	$[1.2690, 0.0883]$	$[1.5059, -0.0063]$

Table 3
State feedback control gains under MRRP.

Scheduling sequence $\hat{\phi}(k)$	Control gains $\bar{K}_{\hat{\phi}(k)} = \text{diag}\{\bar{K}_{1,\hat{\phi}(k)}, \bar{K}_{2,\hat{\phi}(k)}, \bar{K}_{3,\hat{\phi}(k)}, \bar{K}_{4,\hat{\phi}(k)}\}$			
	$\bar{K}_{1,\hat{\phi}(k)}$	$\bar{K}_{2,\hat{\phi}(k)}$	$\bar{K}_{3,\hat{\phi}(k)}$	$\bar{K}_{4,\hat{\phi}(k)}$
1	$[2.8360, -0.8041]$	$[0.0072, 0.0025]$	$[0.0092, 0.0061]$	$[3.8674, -1.0487]$
2	$[3.8674, -1.0487]$	$[0.0092, 0.0061]$	$[0.0072, 0.0025]$	$[2.8360, -0.8041]$

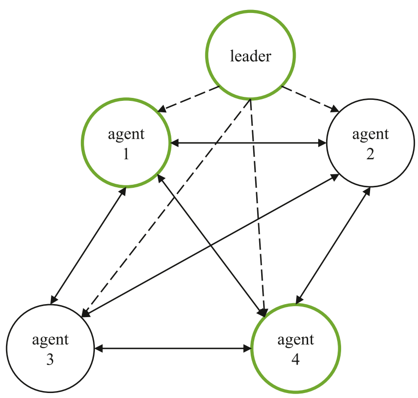

Fig. 12. Communication topology among agents.

4.2. Example 2

As shown in Fig. 12, consider a MAS (4)–(5) with the following parameters:

$$A = \begin{bmatrix} 0.98 & 0.21 \\ -0.22 & 0.97 \end{bmatrix}, \quad B = \begin{bmatrix} 0.2 \\ 0.15 \end{bmatrix},$$

$$L = \begin{bmatrix} 3 & -1 & -1 & -1 \\ -1 & 3 & -1 & -1 \\ -1 & -1 & 3 & -1 \\ -1 & -1 & -1 & 3 \end{bmatrix}, \quad R = \begin{bmatrix} 1 & 0 & 0 & 0 \\ 0 & 1 & 0 & 0 \\ 0 & 0 & 1 & 0 \\ 0 & 0 & 0 & 1 \end{bmatrix}.$$

The controller of the leader agent is given as $u_0(k) = 0$. The parameters in the SMC law are designed as (22) with $\mu = 0.1$, $G = \tilde{B}^T$, $\rho = 3.5$. The agents' initial states are given as $x_0 = [15, 15]^T$, $x_1 = [15, 14]^T$, $x_2 = [16, 16]^T$, $x_3 = [14, 13]^T$, $x_4 = [15, 16]^T$.

Upon solving the optimization problem described in (45), the sliding mode controller gains $K_{\hat{\phi}(k)}$ are achieved and are presented in Table 2, where $\hat{\phi}(k) = 1, 2$ represent two communication topologies of the agents under the MRRP as shown in Fig. 13. Meanwhile, the conventional state feedback controller gains $\bar{K}_{\hat{\phi}(k)}$ are presented in Table 3.

Figs. 14–19 display the simulation results with the sliding mode controller. Fig. 14 shows the trajectories of all agents, where the MAS under the MRRP can achieve consensus tracking. Fig. 15 depicts the scheduling selections of the leader and the follower 1 and 2. Besides, Fig. 16 shows the state error between the leader and each follower. Fig. 17 illustrates the consensus tracking error under the MRRP of the followers. The control signals and sliding variables are depicted in Figs. 18 and 19, respectively. A further comparison with the conventional controller is shown in Figs. 20 and 21. It can be seen that for the nonlinear MASs mentioned in this work, the control effect is not as good as sliding mode control.

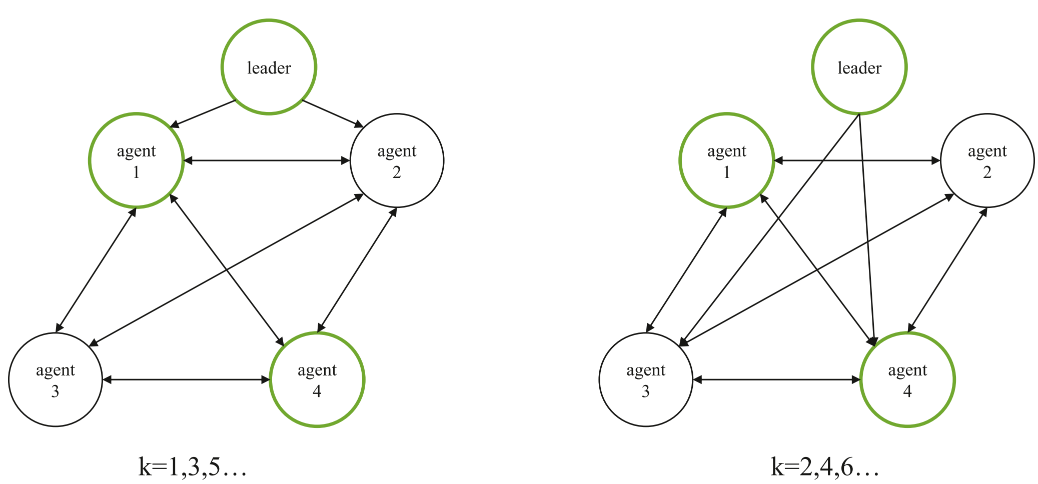

Fig. 13. Communication topology at different times.

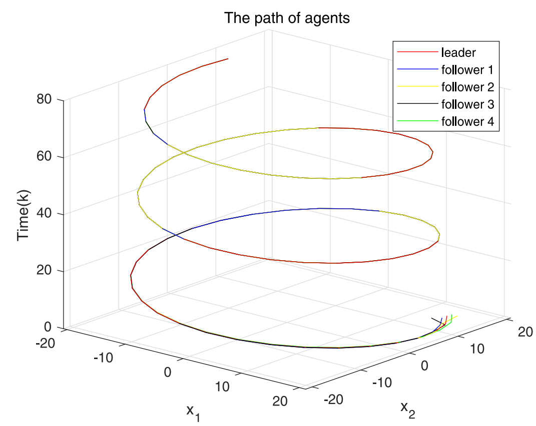

Fig. 14. Motion trajectories.

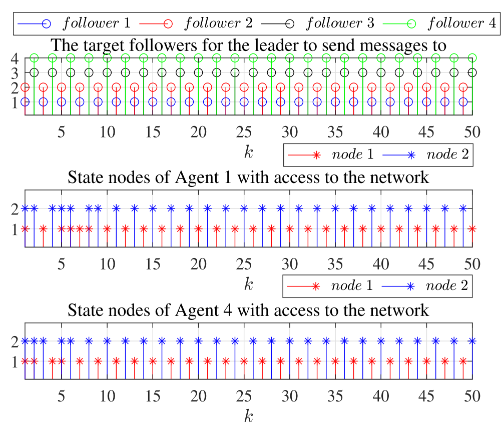

Fig. 15. MRRP scheduling sequence.

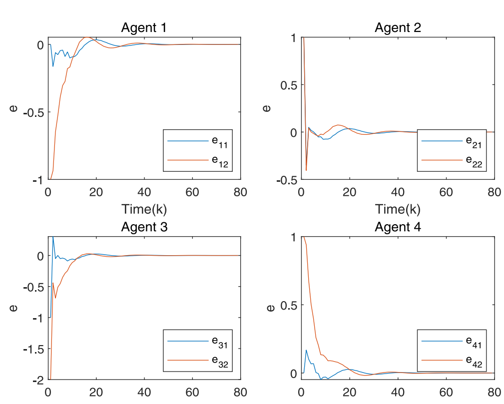

Fig. 16. The state error between followers and leader.

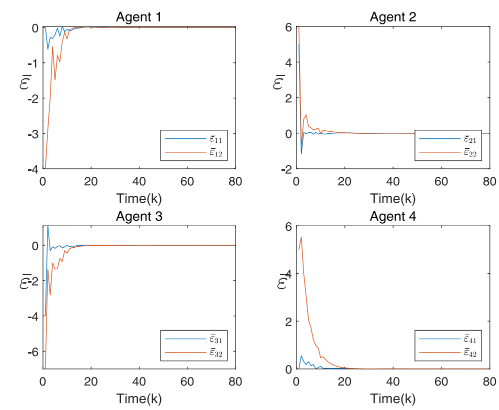

Fig. 17. The consensus error.

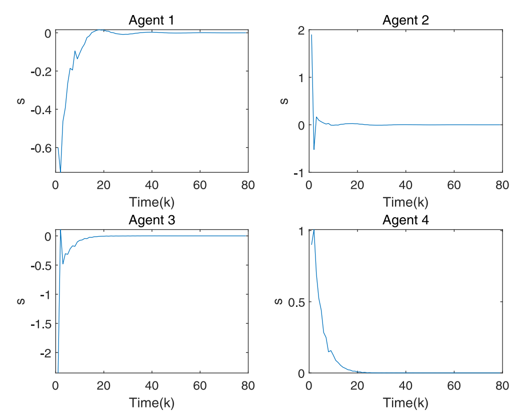

Fig. 18. Sliding variable.

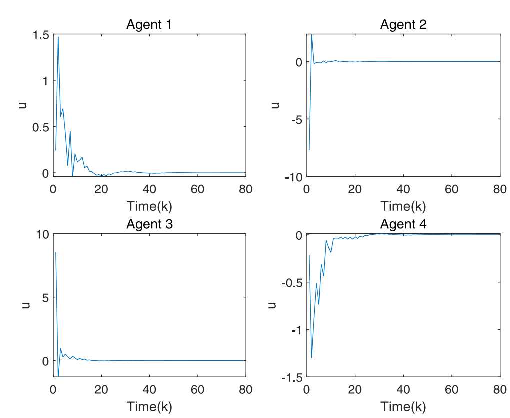

Fig. 19. The control signal of followers.

5. Conclusion

In this work, the consensus tracking issue of the MAS has been investigated via MRRP SMC method. To conserve communication resources and more flexibly schedule information transmission among agents in MASs, the MRRP has been used for the leader and followers. On the one hand, the leader could take turns sending information to the followers around it via the MRRP. On the other hand, the follower could dynamically adjust the number of nodes that send information under the MRRP. Next, consider the impact of the protocol, a distributed token-dependent sliding mode controller has been proposed to achieve the consensus. In this work, we consider the problem of consensus control of MASs with a single leader, and when the system is much larger, especially when it contains multiple leaders, how to use the MRRP to schedule the communication resources of each agent will be a problem worth studying.

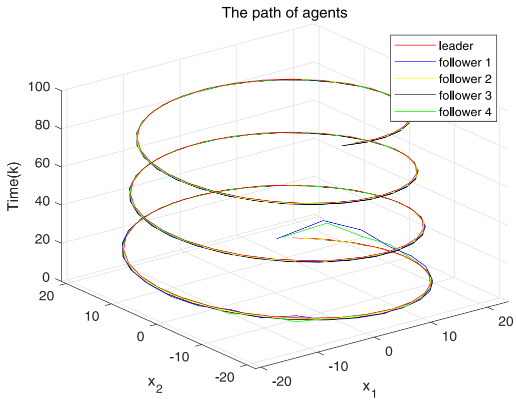

Fig. 20. Motion trajectories with the state-feedback control.

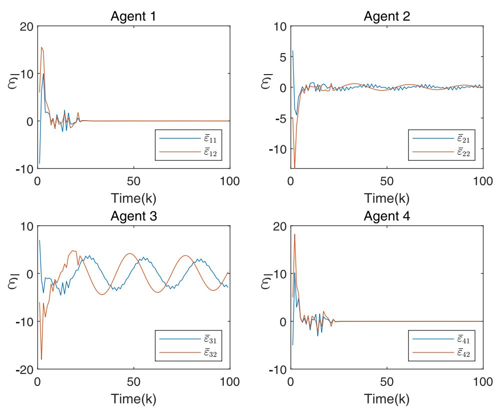

Fig. 21. The consensus error with the state-feedback control.

Declaration of competing interest

The authors declare that they have no known competing financial interests or personal relationships that could have appeared to influence the work reported in this paper.

Data availability

Data sharing not applicable to this article as no datasets were generated or analysed during the current study.

Acknowledgements

This work was supported in part by the Key Projects of the National Natural Science Foundation of China (62333006)

References

[1] M. Xu, K. An, L.H. Vu, et al., Optimizing multi-agent based urban traffic signal control system, J. Intell. Transp. Syst. 23 (4) (2019) 357–369.

[2] J. Terán, J. Aguilar, M. Cerrada, Integration in industrial automation based on multi-agent systems using cultural algorithms for optimizing the coordination mechanisms, Comput. Ind. 91 (2017) 11–23.

[3] C. Huang, S. Weng, D. Yue, et al., Distributed cooperative control of energy storage units in microgrid based on multi-agent consensus method, Electr. Power Syst. Res. 147 (2017) 213–223.

[4] B. Du, S. Li, A new multi-satellite autonomous mission allocation and planning method, Acta Astronaut. 163 (2019) 287–298.

[5] Y. Tang, Z. Deng, Y. Hong, Optimal output consensus of high-order multiagent systems with embedded technique, IEEE Trans. Cybern. 49 (5) (2018) 1768–1779.

[6] X. Li, Y. Tang, H.R. Karimi, Consensus of multi-agent systems via fully distributed event-triggered control, Automatica 116 (2020) 108898.

[7] Z. Yu, W. Zhang, L. Ma, Finite-time consensus for the second-order leader-following nonlinear multi-agent system with event-triggered communication, J. Franklin Inst. B 359 (12) (2022) 6486–6502.

[8] H. Zhang, X. Zhao, L. Zhang, et al., Observer-based adaptive fuzzy hierarchical sliding mode control of uncertain under-actuated switched nonlinear systems with input quantization, Internat. J. Robust Nonlinear Control 32 (14) (2022) 8163–8185.

[9] Y. Hu, H. Yan, H. Zhang, et al., Robust adaptive fixed-time sliding-mode control for uncertain robotic systems with input saturation, IEEE Trans. Cybern. 53 (4) (2022) 2636–2646.

[10] X. Sun, L. Zhang, J. Gu, Neural-network based adaptive sliding mode control for Takagi–Sugeno fuzzy systems, Inform. Sci. 628 (2023) 240–253.

[11] R. Nie, W. Du, Z. Li, et al., Sliding mode-based finite-time consensus tracking control for multi-agent systems under actuator attacks, Inform. Sci. 640 (2023) 118971.

[12] Y. Sun, P. Shi, C.C. Lim, Event-triggered sliding mode scaled consensus control for multi-agent systems, J. Franklin Inst. B 359 (2) (2022) 981–998.

[13] W. Li, Y. Niu, Z. Cao, et al., Sliding mode control for multi-agent systems under stochastic communication protocol, Internat. J. Robust Nonlinear Control 32 (13) (2022) 7522–7535.

[14] H. Ren, Y. Wang, M. Liu, et al., An optimal estimation framework of multi-agent systems with random transport protocol, IEEE Trans. Signal Process. 70 (2022) 2548–2559.

[15] L. Zou, Z. Wang, H. Gao, et al., Finite-horizon H_∞ consensus control of time-varying multiagent systems with stochastic communication protocol, IEEE Trans. Cybern. 47 (8) (2017) 1830–1840.

[16] Y. Yuan, M. Shi, L. Guo, et al., A resilient consensus strategy of near-optimal control for state-saturated multiagent systems with Round-Robin protocol, Internat. J. Robust Nonlinear Control 29 (10) (2019) 3200–3216.

[17] J. Song, F. Han, H. Fu, et al., Finite-horizon distributed H_∞-consensus control of time-varying multi-agent systems with Round-Robin protocol, Neurocomputing 364 (2019) 219–226.

[18] L. Sun, X. Tian, D. Ding, et al., Consensus control of cooperation-competition multi-agent systems with Round-Robin protocols: A set-membership approach, Internat. J. Robust Nonlinear Control 32 (9) (2022) 5005–5022.

[19] W. Chen, D. Ding, H. Dong, et al., Finite-horizon H_∞ bipartite consensus control of cooperation-competition multiagent systems with Round-Robin protocols, IEEE Trans. Cybern. 51 (7) (2020) 3699–3709.

[20] J. Song, Z. Wang, Y. Niu, Static output-feedback sliding mode control under Round-Robin protocol, Internat. J. Robust Nonlinear Control 28 (18) (2018) 5841–5857.

[21] H. Shen, S. Huo, J. Cao, et al., Generalized state estimation for Markovian coupled networks under Round-Robin protocol and redundant channels, IEEE Trans. Cybern. 49 (4) (2018) 1292–1301.

[22] B. Li, Z. Wang, Q.L. Han, et al., Distributed quasiconsensus control for stochastic multiagent systems under Round-Robin protocol and uniform quantization, IEEE Trans. Cybern. 52 (7) (2020) 6721–6732.

[23] J. Li, Y. Niu, J. Song, Sliding mode control design under multiple nodes Round-Robin-like protocol and packet length-dependent lossy network, Automatica 134 (2021) 109942.

[24] Z. Zhang, Y. Niu, Probabilistic-constrained control of interval type-2 T-S fuzzy systems under the multi-node Round-Robin scheduling protocol, J. Franklin Inst. B 360 (9) (2023) 6566–6584.

[25] X. Zhang, L. Liu, G. Feng, Leader-follower consensus of time-varying nonlinear multi-agent systems, Automatica 52 (2015) 8–14.

[26] Y.J. Pan, H. Werner, Z. Huang, et al., Distributed cooperative control of leader-follower multi-agent systems under packet dropouts for quadcopters, Systems Control Lett. 106 (2017) 47–57.

[27] A.H. Tahoun, M. Arafa, Adaptive leader-follower control for nonlinear uncertain multi-agent systems with an uncertain leader and unknown tracking paths, ISA Trans. 131 (2022) 61–72.

[28] L.El. Ghaoui, F. Oustry, A cone complementarity linearization algorithm for static output-feedback and related problems, IEEE Trans. Automat. Control 42 (8) (1997) 1171–1176.